

1 **Psychoacoustic modelling of rotor noise**

2

3 Antonio J. Torija,^{1 a} Zhengguang Li², and Paruchuri Chaitanya,³

4 ¹ *Acoustics Research Centre, University of Salford, Manchester, M5 4WT, United Kingdom*

5 ² *Department of Architecture, Zhejiang University of Science and Technology, Hangzhou, 310023, P.R. China*

6 ³ *Institute of Sound and Vibration Research, University of Southampton, Southampton, SO17 1BJ, United Kingdom*

7

8

9 The aviation sector is rapidly evolving with more electric propulsion systems and a variety of new
10 technologies of Vertical Take-Off and Landing (VTOL) manned and Unmanned Aerial Vehicles
11 (UAVs). Community noise impact is one of the main barriers for the wider adoption of these new
12 vehicles. Within the framework of a perception-driven engineering approach, this paper investigates
13 the relationship between sound quality and first order physical parameters in rotor systems to aid
14 design. Three case studies are considered: (i) contra-rotating vs. single rotor systems, (ii) varying blade
15 diameter and thrust in both contra-rotating and single rotor systems, and (iii) varying rotor-rotor axial
16 spacing in contra-rotating systems. The outcomes of a listening experiment, where participants
17 assessed a series of sound stimuli with varying design parameters, allow a better understanding of the
18 annoyance induced by rotor noise. Further to this, a psychoacoustic annoyance model optimised for
19 rotor noise has been formulated. The model includes a novel psychoacoustic function to account for
20 the perceptual effect of impulsiveness. The significance of the proposed model lies in the
21 quantification of the effects of psychoacoustic factors such as loudness as dominant factor, and also
22 tonality, high frequency content, temporal fluctuations, and impulsiveness on rotor noise annoyance.

23

^a A.J.TorijaMartinez@salford.ac.uk

24 I. INTRODUCTION

25 With the forecast of a substantial expansion of the Unmanned Aerial Vehicles (UAV) sector, the
26 consequent noise generated might lead to a significant problem for public acceptance. The
27 optimisation of UAV designs for minor noise impact on communities requires a complete
28 understanding of sound generation mechanisms of UAV rotors. To date, there is a comprehensive
29 literature on rotorcraft noise, including noise prediction¹⁻³ and annoyance ratings⁴⁻⁶. However, due to
30 the operating conditions of rotorcraft, i.e. high Mach numbers in the transonic regime, this literature
31 might not be of direct application to UAV rotors. During the last few years, researchers have
32 investigated the aeroacoustics of UAV rotors, i.e. with low Reynolds number and low Mach number⁷.
33 Recent research has shown that far-field noise of UAV rotors is mainly characterised by prominent
34 tones at the Blade Passing Frequency (BPF) and its harmonics, and broadband noise at mid and high
35 frequencies^{8,9}.

36 Gojon et al.⁷ conducted an experimental investigation for the acoustic characterization of low
37 Reynolds number isolated rotors. The authors found that for all rotors examined, the far-field
38 frequency spectra were dominated by tonal noise (BPF and its harmonics) and broadband trailing edge
39 noise. Changes in directivities of BPF and overall sound pressure level (OASPL) were observed as a
40 function of rotation speed and number of blades, assumed to be due to phase cancellation of thickness
41 and loading noise sources. Gojon et al.⁷ also discussed the balance between tonal and broadband
42 noise contributions as a function of blade number, i.e., an increase in blade number led to a decrease
43 in BPF amplitude but an increase in broadband noise. Zawodny and Boyd¹⁰ and Whelchel et al.¹¹
44 studied the rotor-airframe interaction for a variety of simplified configurations. More complex
45 configurations like multi-rotors have been investigated by Intaratep et al.¹² and Tinney and Sirohi¹³.
46 Tinney and Sirohi¹³ investigated the effect of the change in blade length on noise emissions in multi-

47 rotors, and also observed how small tip-to-tip distances between rotor blades result in a significant
48 increase in noise emissions due to blade interaction effects.

49 For the specific case of contra-rotating systems, Luan et al.¹⁴ found a strong relationship between the
50 axial rotor spacing and OASPL, with a general trend indicating that OASPL decreases with increase
51 in axial spacing. Torija et al.¹⁵ suggested an optimal rotor axial separation distance (relative to the
52 blade diameter) between 0.2 and 0.4. Chaitanya et al.¹⁶ discussed the reason behind this optimum and
53 attributed it to an optimum balance between the various dominant sources. The potential field
54 interactions were shown to dominate overall noise at separation distances smaller than the optimum
55 distance, while the noise due to tip vortex interaction is dominant for distances greater than the
56 optimum value. Analytical predictions were also performed by Chaitanya et al.¹⁶ to validate their
57 hypothesis. McKay et al.¹⁷ carried out an experimental investigation on noise of contra-rotating
58 systems with varying rotor axial spacing, blade diameter, and blade number. The authors found
59 significant differences in OASPL depending on the specific configuration. The main source of noise
60 identified was potential field interaction tones. It was observed that potential field interaction tones
61 are about 20 dB higher than rotor alone tones at 45 degrees below the contra-rotating system (which
62 is a typical ground observer location with a hovering UAV).

63 However, hitherto, there is not a comprehensive investigation to connect sound quality directly to
64 design parameters of rotary systems. Gwak et al.¹⁸ investigated the Sound Quality Metrics (SQMs)
65 influencing noise annoyance of UAVs. The authors found that the SQMs loudness, sharpness and
66 fluctuation strength are significant factors influencing the annoyance reported for the UAV vehicles
67 tested. Gwak et al.'s¹⁸ research is based on three off the shelf multi-copters, and therefore does not
68 provide a direct link between SQMs and varying design configurations. Torija et al.¹⁵ carried out an
69 analysis based on a series of SQMs and psychoacoustic annoyance (PA) models to define the optimal
70 rotor axial separation distance in contra-rotating systems. These authors investigated the value of

71 several SQMs and PA models¹⁹⁻²¹ as a function of rotors axial spacing, and linked them to the different
72 sound generation mechanisms.

73 SQMs are able to provide a very accurate representation of how the human auditory system response
74 to different sound features. For instance, loudness and sharpness metrics account for the perceived
75 sound intensity and content of high frequency noise respectively. The tonality metric describes how
76 spectral irregularities or discrete tones are perceived. Other SQMs such as fluctuation strength and
77 roughness account for the perception of slow and rapid fluctuations of the sounds level respectively;
78 and impulsiveness describes the perception of short and sudden changes in the sound level (see
79 Boucher et al.⁵ and Torija et al.¹⁵ for further details). A complete understanding on how different
80 design configurations influence the resulting sound quality allows a perception-influenced
81 development of rotary systems, with the potential benefits of more efficient designs to reduce noise
82 impact on communities²².

83 This paper investigates the relationships between primary order design parameters of rotary systems
84 and noise perception. Noise perception is assessed as a function of both existing SQMs and
85 annoyance reported by participants to a comprehensive listening experiment. The specific design
86 parameters investigated are:

- 87 • Contra-rotating vs. single rotor systems (for the same thrust).
- 88 • Different blade diameters and thrust (in contra-rotating and single rotor systems).
- 89 • Different rotor axial spacing in contra-rotating systems (with varying blade diameters).

90 Based on all the data gathered, i.e., participants responses to the series of stimuli encompassing
91 different design parameters, a PA model optimised for rotor noise is formulated and analysed.

92 One of the major contributions of this paper is the understanding of how varying design parameters
93 in rotary systems affect SQMs and overall perceived annoyance. This allows to update and enhance
94 psychoacoustic annoyance models to account for the main psychoacoustic features of rotor noise.

95 Although the aeroacoustics of single and contra-rotating systems (and primary design parameters)
96 have been widely investigated, this paper advances at carrying out a comprehensive analysis of the
97 relationship between physical parameters and perceptual outcomes (e.g., noise annoyance). A new
98 psychoacoustic annoyance model has also been formulated (with a curve fitting procedure) to account
99 for the perceptual effects of impulsiveness, which might be crucial for new rotorcraft vehicles,
100 including multiple rotors configurations and VTOL transition maneuvers.

101 This paper is structured as follows: Section II describes the experimental setup for acoustic
102 measurements; Section III describes the development of the psychoacoustic experiment and the data
103 analysis; Section IV presents and discusses the experimental results and PA model, and are followed
104 by the main conclusions of this work in Section V.

105

106 II. EXPERIMENTAL SET-UP FOR DATA MEASUREMENT

107 An overlapping rotor test rig designed and manufactured at the University of Southampton²³ was used
108 to gather the experimental data for this research. This test rig was assembled with two FOXTECH
109 W61-35 brushless DC (BLDC) (16 poles) 700W motors mounted on a carbon fibre beam. The test
110 rig was operated in two modes, with only a rotor operating (i.e., single rotation) and with two co-axial
111 rotors operating. Commercially available T-Motor 14 inch, 16 inch and 18 inch rotor blades were
112 used both in isolation and also in a co-axial contra-rotating configuration. BLDC motors were
113 controlled with two Maytech 40A-OPTO speed controllers, and Rotations Per Minute were measured
114 with Two Hyperion HP-EM2-TACHBL sensors (see Torija et al. (2021)¹⁵ for further details).

115 The overlapping rig allowed manipulation of the rotary system in rotor axial separation distance z/D
116 (with D as the rotor diameter). Overall, sixteen z/D positions were measured: 0.05, 0.075, 0.1, 0.125,
117 0.15, 0.175, 0.2, 0.25, 0.3, 0.35, 0.4, 0.45, 0.5, 0.6, 0.8 and 1.0. Note that all measurements were taken
118 with the lower rotor plane was at least three rotor diameters away from the ground with anechoic

119 wedges beneath. In this research, only z/D positions 0.05, 0.1, 0.2, 0.4, 0.6 and 1.0 are considered for
120 the listening experiment and further analysis.

121 The combined thrust of the contra-rotating system was varied from 2 to 20N in steps of 2N. In
122 additions, for comparison the single-rotor propulsion system was varied from 1 to 10N in steps of
123 1N. In this research, only data measured at 6N and 10N (single rotation), and 6N, 10N and 16N
124 (contra-rotation) is considered for the listening experiment and further analysis.

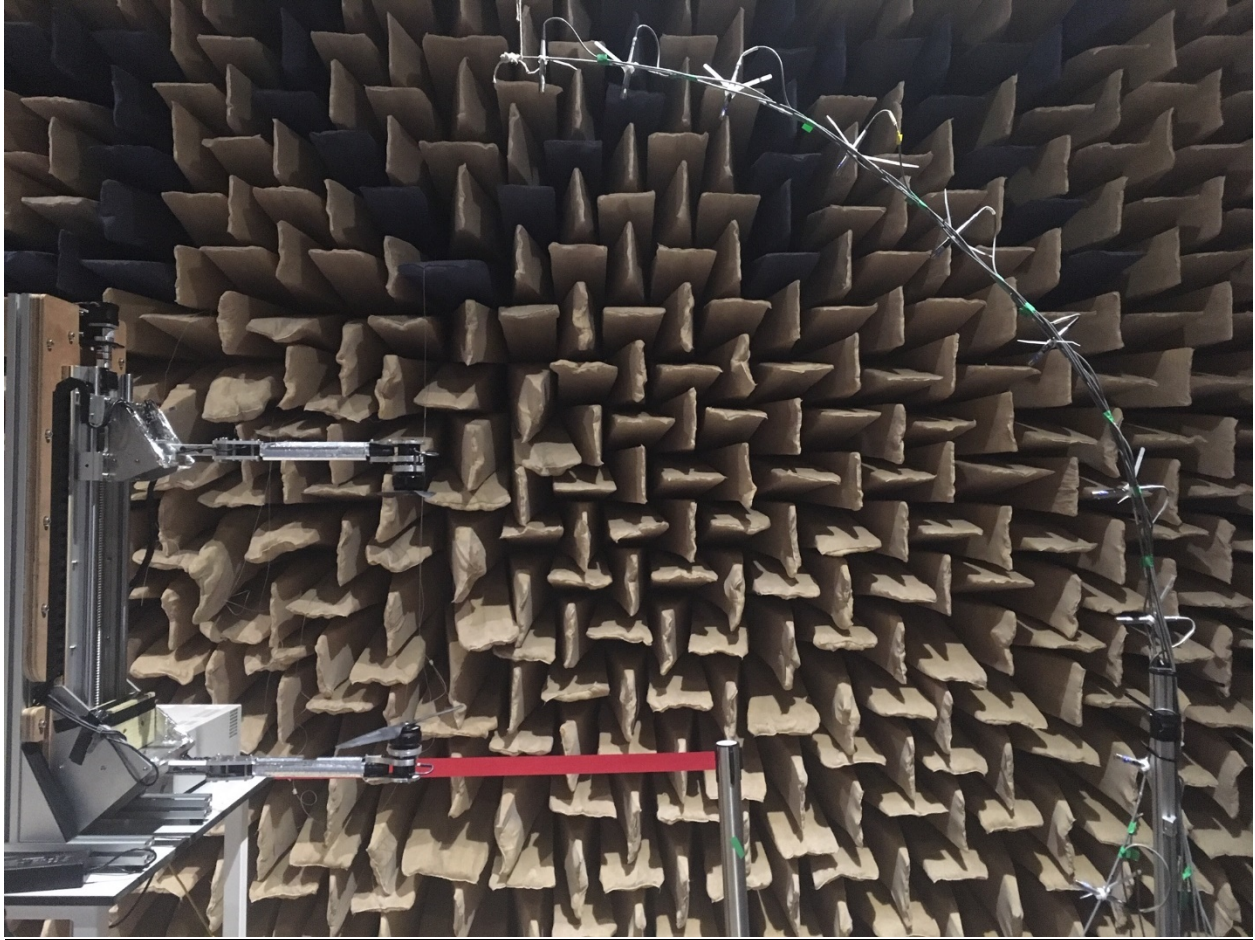
125

126 III. DEVELOPMENT OF PSYCHOACOUSTIC EXPERIMENT AND DATA 127 ANALYSIS

128 A. Sound recording

129 Sound samples for the listening experiment and psychoacoustic analysis were extracted from a series
130 of far-field noise measurements made for the different configurations described in section II. The
131 far-field measurements were carried out at the Institute of Sound and Vibration Research's open-jet
132 wind tunnel facility, with the overlapping rotor test rig placed within an anechoic chamber (dimensions
133 = 8 m \times 8 m \times 8 m, and cut-off frequency of 80 Hz).

134 An array of 10 $\frac{1}{2}$ in. condenser microphones (B&K type 4189) was used for the far-field
135 measurements (see Figure 1). This array of microphones was located at a constant radial distance of
136 2.5 m from the centre of the propellers. The microphones were placed at emission angles of between
137 about 10 degrees and 100 degrees, measured relative to the bottom rotor. Note that, only data
138 measured at emission angles 10 degrees and 85 degrees was considered for the listening experiment
139 and psychoacoustic analysis. Ten degrees and 85 degrees are roughly the azimuthal angles with
140 maximum and minimum emission respectively for potential field interaction tones.^{15,17}



141

142 Figure 1. Experimental setup. (color online)

143

144 These far-field noise measurements were carried out for 10 s duration at a sampling frequency of 50
145 kHz. The frequency spectra were obtained with a window size of 1024 data points, with corresponds
146 to a frequency resolution of 48.83 Hz and a Bandwidth-Time product of about 500. This is considered
147 sufficient to ensure negligible variance in the spectra estimated at this frequency resolution.

148 **B. Sound stimuli**

149 Ninety-two stimuli, including 84 test stimuli, 7 master scaling stimuli and 1 reference stimulus, were
150 used in the listening experiment. As described in section II.A, these sound stimuli were selected from
151 the far-field noise database recorded, to account for a wide range of design parameters in a rotary
152 system. This was deemed to be essential to develop a psychoacoustic annoyance model able to

153 account for the perceptual effects of the major features of rotor noise. The list of sound stimuli used
 154 in the listening experiment are summarized in Table I.

155

156 Table I. Summary of sound stimuli used in the listening experiment.

Stimuli	Rotary System	Thrust (N)	Blade diameter (inch)	Axial spacing (z/D)	Emission angles (degrees)	Numbers of stimuli
Reference stimulus	Contra-rotating	16	16	0.15	100	1
Master scaling stimuli	Contra-rotating	10	16	0.075	20	7*
Test stimuli in Part 1	Contra-rotating	6 10	16	0.05, 0.1, 0.2, 0.4, 0.6, 1	10 85	24
	Single-rotor	6 10	14 16 18	-	10 85	12
Test stimuli in Part 2	Contra-rotating	16	16	0.05, 0.1, 0.2, 0.4, 0.6, 1	10 85	12
	Contra-rotating	16	14 16 18	0.05, 0.1, 0.2, 0.4, 0.6, 1	10 85	36

157 *These 7 stimuli were from the same sound recording but with different sound levels after adjustment
 158 in amplitude (to derive a master-scale, see Section III.F).

159

160 The duration of all stimuli was 3 s. This stimuli length was carefully selected to be long enough for
 161 the participants to be able to decide and report perceived annoyance while minimizing participant's
 162 fatigue.²⁴ Both to increase the realism of the scenarios presented (i.e., vehicle hovering) and minimise
 163 the risk of sound exposure, the sound level of all the stimuli were normalised to the level at the position
 164 of 50 m from the centre of the propellers, according to the sound propagation law of a point source.
 165 The target sound level (L_{Aeq}) of the reference stimulus was set at 51.8dBA. This specific L_{Aeq} was

166 chosen as it is the median (L_{Aeq}) value of all the test sounds used in the subjective experiment. The
167 reference stimulus was selected because it has an ‘average’ loudness (considering all the test sounds),
168 and it does have any significantly perceivable psychoacoustic feature (i.e., tonality, amplitude
169 modulation, roughness, etc.). The 7 master scaling stimuli were generated from the same stimulus by
170 modifying its sound level (L_{Aeq}) to 40.1dBA ~ 70.1dBA, in increments of 5dB. These 7 master scaling
171 stimuli covered approximately the whole range of L_{Aeq} of all the test stimuli used, which ranged from
172 39dBA to 68.9dBA. The sound used to synthesise the 7 master scaling stimuli was dominated by the
173 present of potential field interaction tones, as the main sound generation mechanisms in contra-
174 rotating systems with rotors closely spaced^{15,16}. A clearly dominant acoustic feature with sound levels
175 varying widely, to cover the whole range of test sounds, allowed the derivation of a linear master scale
176 as described in section III.F.

177 **C. Experimental setup**

178 The hardware setup used for the listening experiment consisted of a powerful desktop computer (Intel
179 Core i7-2600 CPU @3.40 GHz, 16.0 GB RAM, 64-bit Windows 10 Operating System) with a USB
180 DAC/headphone amplifier (Audioquest, DragonFly Cobalt v1.0) and a pair of open back headphones
181 (Audio-Technica, ATH-M70x). The listening tests were carried out in a very quiet environment (i.e.,
182 a lab room of Zhejiang University of Science and Technology, with the background sound level of
183 21.6 dBA), with no interference from outside in order to avoid distractions.

184 The test was entirely automated via a bespoke MATLAB code. The volume level on the desktop was
185 always set to maximum, with MATLAB controlling the playback volume to ensure consistency.

186 The headphone reproduction was calibrated in sound pressure level using an artificial head (HEAD
187 acoustics GmbH, HMS IV.0) to the corresponding target sound levels, without altering neither
188 temporal nor spectral characteristics.

189 **D. Participants**

190 The listening tests were undertaken by 33 healthy participants (17 males and 16 females) aged between
191 20 and 23 years old (mean age = 21.2, standard deviation = 0.8) who were recruited by advertisement
192 within Zhejiang University of Science and Technology. A thank you gift of ¥50 for taking part was
193 used to incentivize participation in the listening tests. Prior to participating in the listening test, each
194 participant was required to confirm normal hearing ability and asked to fill out a consent form.
195 Responses from 4 participants were discarded due to severe inconsistencies in their responses.
196 Therefore, the responses of perceived annoyance reported by these 4 participants were not considered
197 in the psychoacoustic analysis carried out. Finally, responses from 29 participants (14 males and 15
198 females) aged between 20 and 23 years old (mean age = 21.1, standard deviation = 0.9) were analysed
199 in this paper.

200 **E. Experimental procedure**

201 The listening experiment started with the participants being presented 7 sounds to derive a master
202 scale. As described above, these sounds were the same sound sample (see Table I for details) with 7
203 different sound levels. The goal of deriving a master scale is to scale and calibrate the scales used by
204 different participants to a common master scale.²⁵
205 After the master scale part was finished, the listening experiment involved a series of assessment task
206 groups, where the participants reported their perception of noise annoyance induced by the sounds
207 they heard, using a relative-number magnitude estimation scale. The relative magnitude estimation
208 method²⁶ was selected for reporting the perceived noise annoyance as it provides outcomes in a
209 continuous scale, thus simplifying the derivation of the psychoacoustic annoyance model. The
210 participants were asked to rate the perceived noise annoyance of each test sound numerically against
211 a defined reference stimulus which was given an arbitrary rating of 100.

212 In order to reduce participant's fatigue, the listening experiment was divided into two parts. In part 1,
213 the 36 stimuli (see Table I) were randomly allocated into 9 groups. In part 2, there were 48 stimuli
214 (see Table I) which were randomly grouped into 12 groups. In each group, 5 stimuli were presented,
215 including 1 reference stimulus and 4 test stimuli. The reference stimulus was the same for all groups,
216 and it was presented in first place. After listening to the reference stimulus, the 4 test stimuli randomly
217 selected were presented sequentially to the participants, with a gap of 2s in between stimulus. The
218 participants were required to type their responses after they have heard each test stimulus. They were
219 asked to rate numerically each test stimulus, so that the numerical difference between such stimulus
220 and the reference stimulus (allocated noise annoyance rating of 100) reflected the perceived difference
221 in annoyance. Note that no restriction on number values was indicated to the participants. During the
222 assessment process, the participants were allowed to listen to each stimulus as many times as they
223 required, and change their response until the final assessment was decided. Once a given group of
224 stimuli was rated, the participant continued with another group until all test stimuli were rated. The
225 duration of the whole listening experiment, including master scaling phase, part 1 and part 2 was about
226 30 min.

227

228 **F. Master scaling**

229 The measurement of noise-induced annoyance is always a contextually based dynamic process.²⁷
230 Different participants are likely to give different magnitude estimates of noise annoyance to the same
231 stimulus, according to their own scaling context. In order to address this issue, 7 reference stimuli
232 with varying sound level were presented to the participants to help them define their own scaling
233 context. The reported annoyance for these reference stimuli was used to control for the individual
234 participants' choice-of-number behaviour in scaling the test sounds. Following Berglund (2013)²⁸,

235 each individual participant’s annoyance scale was calibrated with the reference to a common master
236 scale.

237 According to De Coensel et al. (2007)²⁵, individual’s response to noise annoyance and the sound level
238 of the stimuli fit according to Equation 1.

$$239 \qquad R = aL_p + b \qquad \text{(Equation 1)}$$

240
241 Where R is the reported annoyance, L_p is the sound level of the stimulus, and a and b are constants
242 which are different for each participant, and therefore characterize their individual’s scaling context.

243 Note that the choice of the psychophysical function to build the common master scale (Equation 1)
244 was based on previous research where noise annoyance values were scaled in a similar manner.²⁵

245 The response to the 7 master scaling stimuli in this listening experiment were used to build each
246 participant’s annoyance scaling, according to Equation 1. The common master scale was built based
247 on the average value of noise annoyance reported by all valid participants (i.e., after discarding the
248 responses of participants with severe inconsistencies in their responses, see section III.D). By the aid
249 of the reference to the common master scale, each individual participant’s annoyance scale was
250 calibrated using Equation 2.

$$251 \qquad R_i = \frac{a_i(R_0 - b_0)}{a_0} + b_i \qquad \text{(Equation 2)}$$

252 Where R_i and R_0 are the reported annoyance to a stimulus in the scaling of participant i and in the
253 common master scaling respectively, a_i and b_i are the constants characterizing individual’s scaling, a_0
254 and b_0 are the constants characterising the common master scaling.

255 **G. Data analysis**

256 A threshold of correlation coefficient between the reported annoyance and L_{Aeq} for the master scaling
257 stimuli was set for the participants’ responses to be considered for the psychoacoustic analysis. As
258 indicated above, 4 participants’ data were discarded due to the low correlation coefficient (R^2 was

259 lower than 0.6) between reported annoyance and L_{Aeq} for the 7 stimuli used in the master scaling part.
260 The mean of all 29 valid participants' response was calculated as the final annoyance of each stimulus.
261 The SQMs [including loudness in sone, sharpness in acum, fluctuation strength in vacil, roughness in
262 asper, impulsiveness in Impulsiveness Units (IU), and tonality in Tonality Units (TU)] of all sound
263 samples were calculated with ArtemiS software (HEAD acoustics GmbH). For further details about
264 the specific methods implemented, see Torija et al. (2021).¹⁵ As recommended in the literature²⁰, the
265 5th percentile of each SQM was used for the psychoacoustic analysis. As the sound stimuli were
266 constant in amplitude, it was assumed that the findings of the psychoacoustic analysis are non-
267 dependent of the given statistical parameter used as output of the SQM. The first 0.5 s of each sound
268 stimulus were ignored in the calculation of the 5th percentile of each SQM, in order to avoid the
269 transient effect of the digital filters implemented in the algorithms to calculate the SQMs.
270 All the statistical analyses, presented in section IV, were carried out with the statistical package IBM
271 SPSS Statistics 25.

272

273 **IV. RESULTS AND DISCUSSION**

274 **A. Contra-rotation vs. single rotor**

275 The contra-rotating and single rotor systems were compared in terms of reported annoyance and
276 value of SQMs. The 16 in. blade diameter configuration was selected, and comparisons were made
277 for the 6 N and 10 N thrust settings and 10 degrees and 85 degrees emission angles. For each thrust
278 setting and emission angle, seven cases were considered: i.e., six rotor-rotor axial spacings ($z/D =$
279 0.05, 0.1, 0.2, 0.4, 0.6, 1.0) and single rotor configuration.

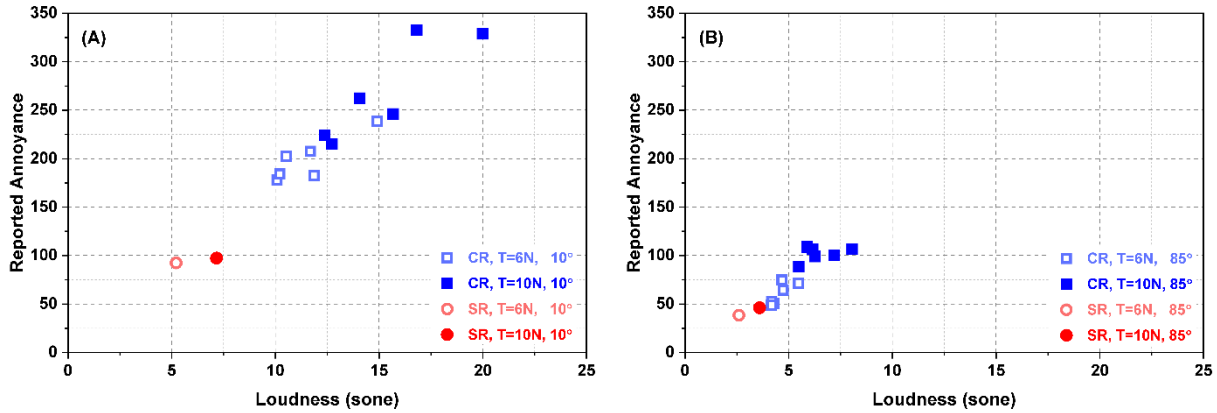
280 An Independent-Samples Mann-Whitney U Test, carried out for the configurations and cases
281 described above, showed that there are statistically significant differences ($p < 0.05$) between the

282 contra-rotating and single rotor systems in terms of reported annoyance ($p = 0.024$), Loudness ($p =$
283 0.029), Roughness ($p = 0.042$) and Fluctuation Strength ($p = 0.019$). Even though the same thrust is
284 generated, the loudness of the single rotor is significantly lower than the loudness of the contra-
285 rotating system (even for the psychoacoustic optimal axial spacing¹⁵). Rotor-rotor interaction also
286 leads to higher values of Roughness and Fluctuation Strength for the contra-rotating system,
287 compared to the single rotor. Roughness has significant values at higher rotor-rotor axial spacings
288 (i.e., $z/D = 0.6, 1.0$), while Fluctuation Strength has the highest values either at reduced rotor-rotor
289 axial spacings ($z/D = 0.05, 0.1$) or large rotor-rotor axial spacings (i.e., $z/D = 0.6, 1.0$). This has been
290 previously identified by Torija et al. (2021)¹⁵ and attributed to the enhancement of turbulence-rotor
291 interaction noise at larger rotor-rotor axial spacing. Similarly, at lower rotor-rotor axial spacing
292 distances the dominant noise generating mechanism is due to the potential field interactions^{15,17}. Note
293 that one of the main perceptual differences when listening to contra-rotating sounds, as compared to
294 single rotors, is the beating sound (i.e., a sound with low frequency amplitude modulation). The
295 annoyance reported for the single rotor case is 48% (6 N / 10 degrees), 24% (6 N / 85 degrees), 57%
296 (10 N / 10 degrees) and 48% (10 N / 85 degrees) lower than the annoyance reported for the rotor-
297 rotor axial spacing $z/D = 0.2$ (psychoacoustic optimal axial spacing¹⁵).

298 In Figure 2, it can be seen that the differences in reported annoyance (i.e., inter-individual average
299 value for each test sound) and Loudness between the contra-rotating and single rotor systems are
300 higher at 10 degrees (i.e. emission angle with high amplitude of potential field interaction tones^{15,17})
301 than at 85 degrees, where the emission of rotor alone tones dominate.

302 It should be noted that plots for Roughness and Fluctuation Strength have not been included in Figure
303 2, as the association between these two SQMs and reported annoyance is influenced by Loudness (as
304 a confounding factor). See section IV.D for further details.

305



306

307 Figure 2. Reported annoyance (i.e., inter-individual average value for each test sound) vs. Loudness,
 308 for emission angle of 10 degrees (A) and 85 degrees (B). Configuration with 16 in blade diameter, and
 309 thrust setting of 6 N and 10 N. (color online)

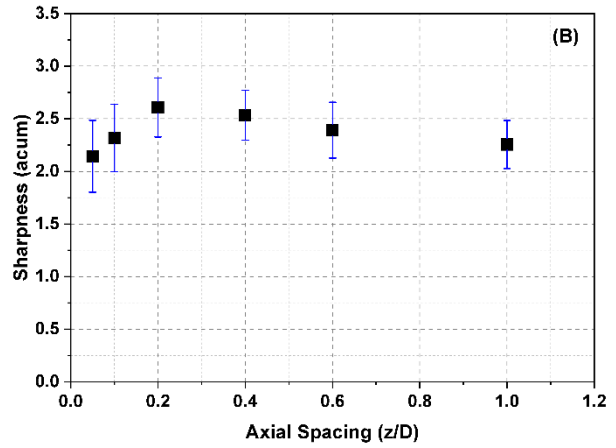
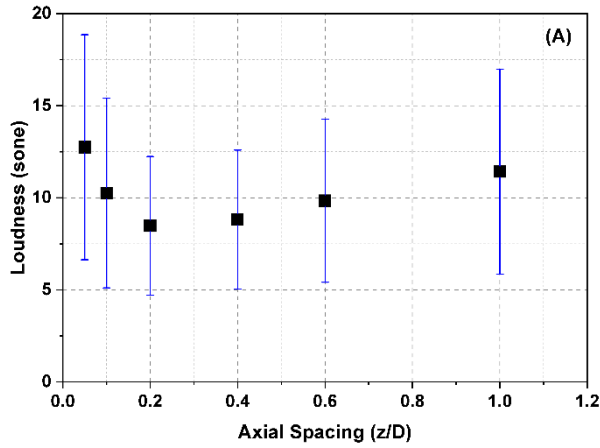
310

311 **B. Psychoacoustic metrics and annoyance vs. rotor spacing**

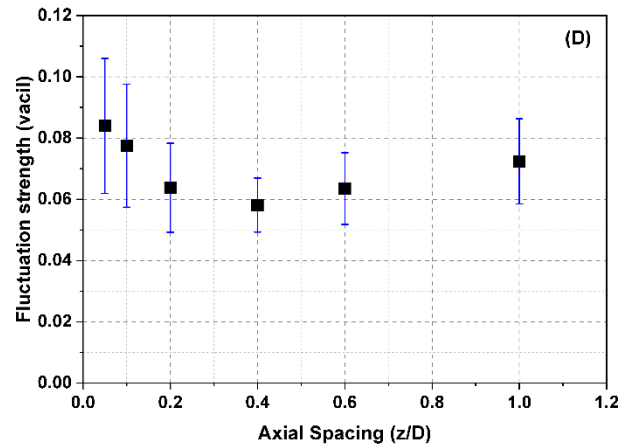
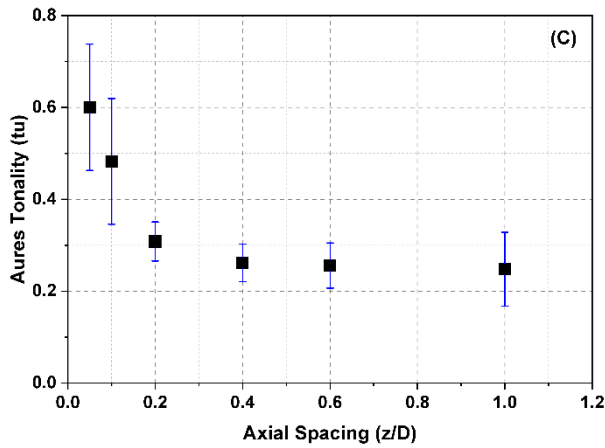
312 The changes in SQMs with varying rotor-rotor axial spacing (z/D) in the contra-rotating system was
 313 investigated. Figure 3 (A) to Figure 3 (F) displays the values of Loudness, Sharpness, Aures Tonality,
 314 Fluctuation Strength, Roughness and Impulsiveness for rotor-rotor axial spacings (z/D) 0.05, 0.1, 0.2,
 315 0.4, 0.6 and 1.0. Figure 3 shows the mean values and standard deviations bars for the data including
 316 14 in, 16 in and 18 in blade diameter; 6 N, 10 N and 16 N thrust settings; and emission angles 10
 317 degrees and 85 degrees.

318 As described in Torija et al. (2021)¹⁵, at reduced rotor-rotor axial spacing the dominant noise source
 319 in contra-rotating systems are potential field interaction tones. As the axial spacing between the rotors
 320 increases, the magnitude of such potential field interaction tones becomes smaller, and consequently
 321 the overall Loudness (Figure 3 (A)) and Aures Tonality (Figure 3 (C)) is significantly reduced, reaching
 322 minimum values at about $z/D = 0.2 - 0.4$. This decrease in the amplitude of potential field interaction
 323 tones has two other effects: the beating effects (or low frequency amplitude modulation) due to the
 324 interaction between rotors diminishes (see Figure 3 (D)) for a reduction of Fluctuation Strength until

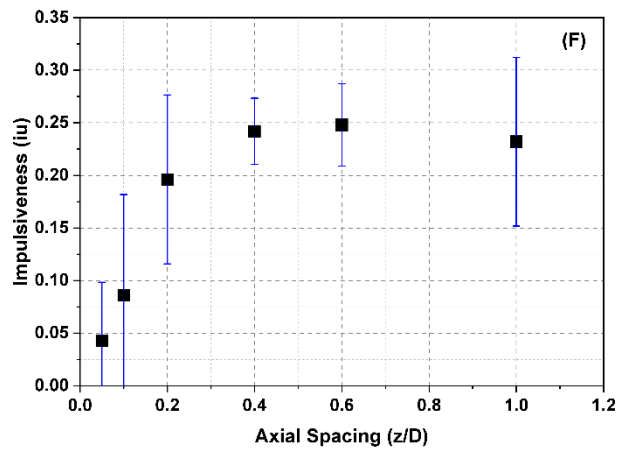
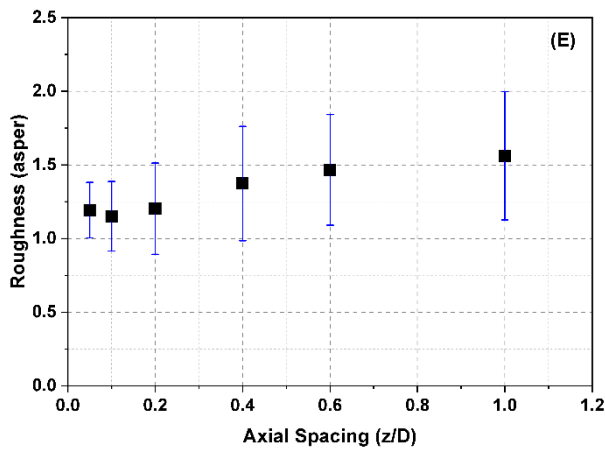
325 $z/d = 0.4$ as rotor-rotor axial spacing increases); with a lesser amplitude of potential field interaction
326 tones (i.e., dominant noise source) at about $z/D = 0.2 - 0.4$, the contribution of high frequency tonal
327 and broadband components becomes more important, and therefore an increase in Sharpness is
328 observed (see Figure 3 (B)). At larger rotor-rotor axial spacing the dominant noise source in contra-
329 rotating systems are enhanced turbulence-rotor blade interactions. This is illustrated by the significant
330 increase of both Roughness (Figure 3 (E)) and Impulsiveness (Figure 3 (F)) as the axial spacing
331 between rotors increases. These two SQMs are strongly linked to each other²⁹ and have been found
332 to be able to account for the unsteadiness in rotor noise.¹⁵ This added unsteady turbulence-rotor
333 blade interaction noise causes an increase in Loudness as the rotors move apart from each other.



334



335



336

337 Figure 3. The 5th percentiles of Loudness (A), Sharpness (B), Aures Tonality (C), Fluctuation Strength
 338 (D), Roughness (E) and Impulsiveness (F) as a function of rotor-rotor axial spacing (z/D). Standard

339 deviation bars accounts for varying configurations: 14 in, 16 in and 18 in blade diameter; 6 N, 10 N
340 and 16 N thrust settings; and emission angles 10 degrees and 85 degrees. (color online)

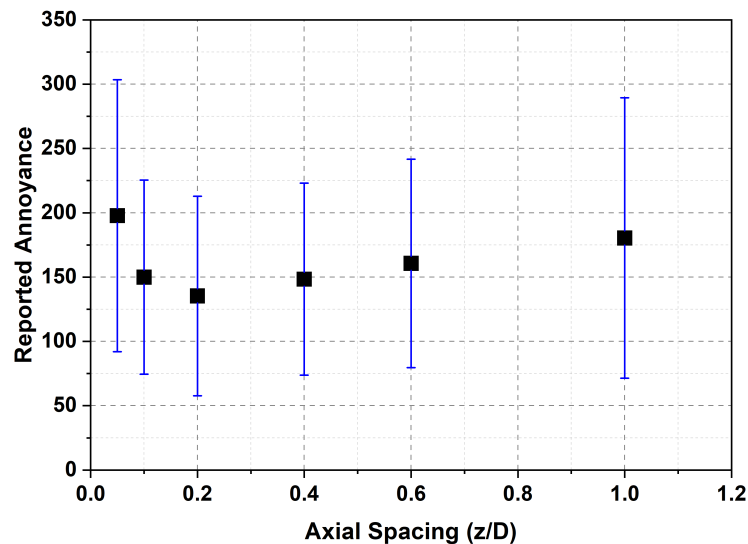
341

342 Figure 4. Reported annoyance as a function of rotor-rotor axial spacing. Standard deviation bars
343 accounts for varying configurations: 14 in, 16 in and 18 in blade diameter; 6 N, 10 N and 16 N
344 thrust settings; and emission angles 10 degrees and 85 degrees. (color online)

345 *shows the inter-individual average values (and standard deviation bars accounting for varying configurations: 14 in, 16 in and*
346 *18 in blade diameter; 6 N, 10 N and 16 N thrust settings; and emission angles 10 degrees and 85 degrees) of the reported*
347 *annoyance as a function of rotor-rotor axial spacing (z/D). As can be seen in Figure 4. Reported annoyance as a*
348 function of rotor-rotor axial spacing. Standard deviation bars accounts for varying
349 configurations: 14 in, 16 in and 18 in blade diameter; 6 N, 10 N and 16 N thrust settings; and
350 emission angles 10 degrees and 85 degrees. (color online)

351 , the participants of the subjective experiment found the sound samples at an axial spacing $z/D = 0.2$
352 as the less annoying. The presence of potential field interaction tones at reduced rotor-rotor axial
353 spacing, and unsteady turbulence-rotor blade interaction at larger spacings, seemed to be picked up
354 by participants responses. The trend of reported annoyance as a function of axial spacing between
355 rotors almost matches the Loudness vs. axial spacing pattern. This seems to suggest that the
356 participants responses were mainly driven by Loudness, although further analysis is needed (see
357 Section IV. D). Exploring Figure 3, it can be seen that participants' responses might somehow be
358 influenced the significant reduction of Aures Tonality (after $z/D = 0.2$), and the Fluctuation Strength
359 vs. axial spacing pattern (with the lowest values at $z/D = 0.2-0.4$). This might suggest that Loudness
360 is the main contributor for the reported annoyance for the contra-rotating system investigated,
361 although the influence of Tonality and low frequency amplitude modulation (due to beating effects

362 between rotors) should also be considered. However, the specific contribution of Tonality and
363 Fluctuation Strength to reported annoyance should be interpreted with caution as explained in section
364 IV.D.



365
366 Figure 4. Reported annoyance as a function of rotor-rotor axial spacing. Standard deviation bars
367 accounts for varying configurations: 14 in, 16 in and 18 in blade diameter; 6 N, 10 N and 16 N
368 thrust settings; and emission angles 10 degrees and 85 degrees. (color online)

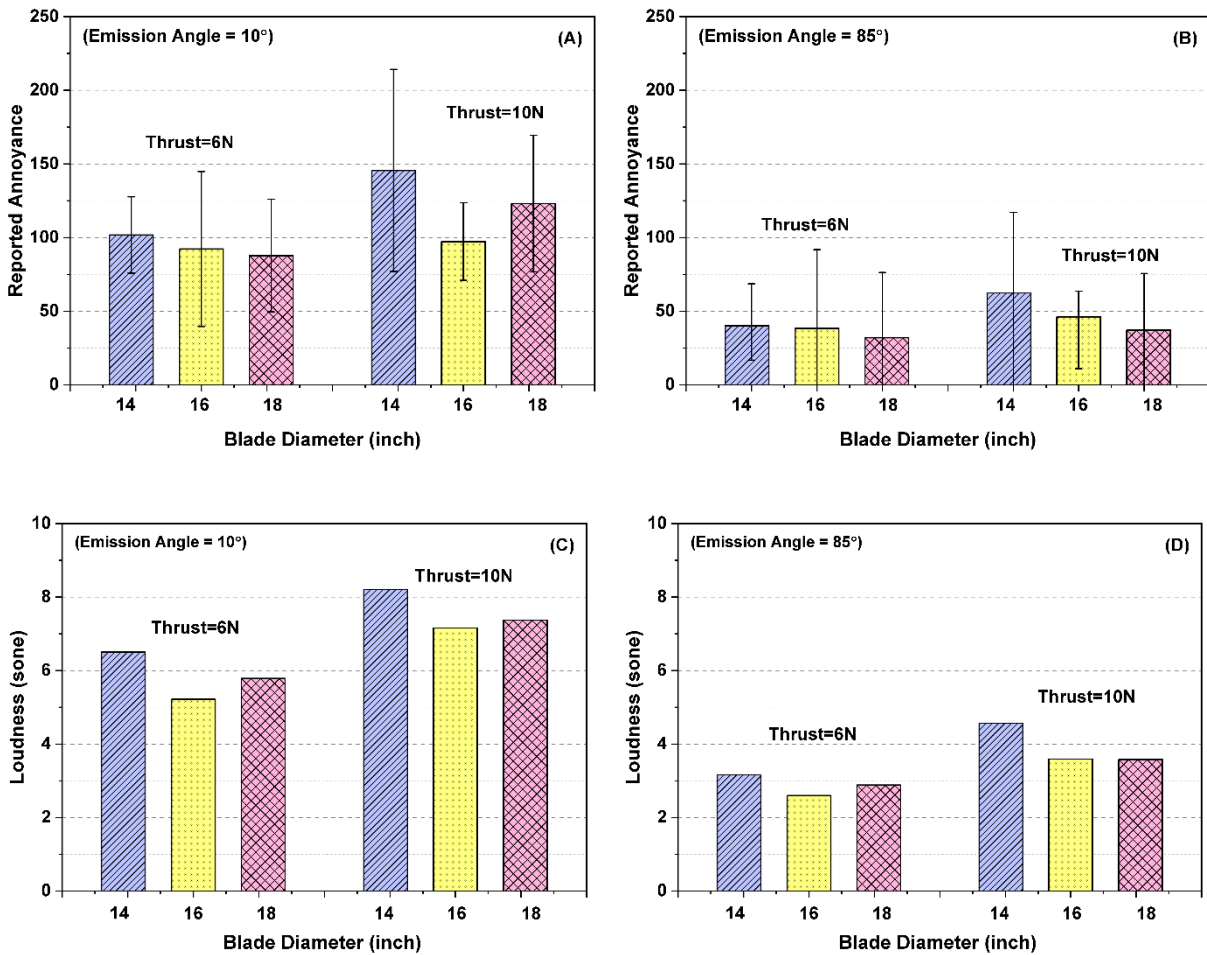
369
370 **C. Psychoacoustic metrics and annoyance vs. blade diameter**

371 Figure 5 shows the changes in Loudness and reported annoyance (i.e., inter-individual average values
372 per test sound) for the three blade diameters (i.e., 14 in, 16 in, and 18 in) considered in this research
373 for the single rotor configuration. Results are shown for thrust settings of 6 N and 10 N, and for
374 emission angles of 10 degrees and 85 degrees. In general, as seen in Figure 5, reported annoyance
375 diminishes with the increase of blade diameter. This is in line with the decrease of Loudness with
376 blade diameter. Figure 5 shows a reduction of Loudness from 14 in blade diameter to 16-18 in blade
377 diameters. Table II also displays the average value (accounting for data for thrust settings of 6 N and

378 10 N, and for emission angles of 10 degrees and 85 degrees) for the SQMs Sharpness, Aures Tonality,
379 Fluctuation Strength, Roughness and Impulsiveness as a function of blade diameter. As the blade
380 diameter increases from 14 in to 18 in, there is a slight reduction of Sharpness and an important
381 decrease of Aures Tonality. The reduction of Loudness seems to drive the responses of the
382 participants for lower reported annoyance as rotor blade diameter increases.

383 For a given thrust, an increase in blade diameter leads to a reduction of blade loading. As stated by
384 Tinney and Sarohi (2018)¹³, an increase of rotor blade diameter can ensure the generation of the same
385 thrust levels with lower rotational speed, leading this to an important reduction of thickness and
386 loading noise. That reduction in the rotational speed of the single rotor system causes a displacement
387 of the BPF (and its harmonics) towards the low frequency region, with the consequent reduction in
388 Sharpness and Aures Tonality. At the same time, as shown in Table II, the increase in rotor blade
389 diameters leads to an increase in Roughness and Impulsiveness, which might indicate an increase in
390 broadband noise due to interaction of boundary layer with blade trailing edge and the interaction of
391 turbulent wake with neighboring propeller blade. Larger diameter propeller blades have larger chord
392 and hence the boundary layer thickness increases which results in increases in broadband noise.
393 Chaitanya et. al. (2021)¹⁶ argues that for a single rotor, the radiated acoustic power varies as $\mathbf{N}^{5.5}\mathbf{D}^3$,
394 where \mathbf{N} is the rotational speed and \mathbf{D} is the diameter of the propeller. The total noise therefore
395 follows a thrust scaling law of $\mathbf{T}^{2.75}$ and velocity scaling law of $\mathbf{U}^{5.5}$, which is identical to the scaling
396 law characteristics of aerofoil leading edge noise. With the increase in propeller diameter, to maintain
397 the same thrust the rotational speed (\mathbf{N}) needs to be reduced, which results in reduction of radiated
398 noise following scaling law $\mathbf{N}^{5.5}\mathbf{D}^3$. With larger diameter propellers, the BPF occurs at lower
399 frequencies and hence this results in lower sharpness compared with smaller diameter propellers. It is
400 worth noting here that in this scaling with rotational speed, \mathbf{N} is predominant compared to diameter
401 \mathbf{D} . The reason behind this may requires further work.

402 For the case of a thrust setting of 10 N at the emission angle 10 degrees, the value of reported
 403 annoyance for the 16 in blade diameter is lower than for the 18 in blade diameter. This might be
 404 attributable to the slightly lower Loudness of the 16 in blade diameter, compared to the Loudness of
 405 the 18 in blade diameter.
 406



407
 408
 409 Figure 5. Reported annoyance (inter-individual average value) (A and B) and Loudness (C and D) as
 410 a function of blade diameter for the single rotor system. Data is displayed for 6 N and 10 N thrust
 411 settings and emission angles = 10 degrees (left) and 85 degrees (right). *Note that negative values in
 412 SD bars are due to reported data converted to a common master scale of annoyance (see section
 413 III.F) (color online)

414

415 Table II. Average values of Sharpness, Aures Tonality, Fluctuation Strength, Roughness and
416 Impulsiveness as a function of blade diameter for the single rotor system. These average values
417 include data for thrust settings of 6 N and 10 N, and for emission angles of 10 degrees and 85
418 degrees.

	Blade diameter = 14 in	Blade diameter = 16 in	Blade diameter = 18 in
Sharpness (acum)	2.72	2.60	2.60
Aures Tonality (tu)	0.45	0.48	0.35
Fluctuation Strength (vacil)	0.05	0.04	0.05
Roughness (asper)	0.66	0.70	0.80
Impulsiveness (iu)	0.10	0.16	0.23

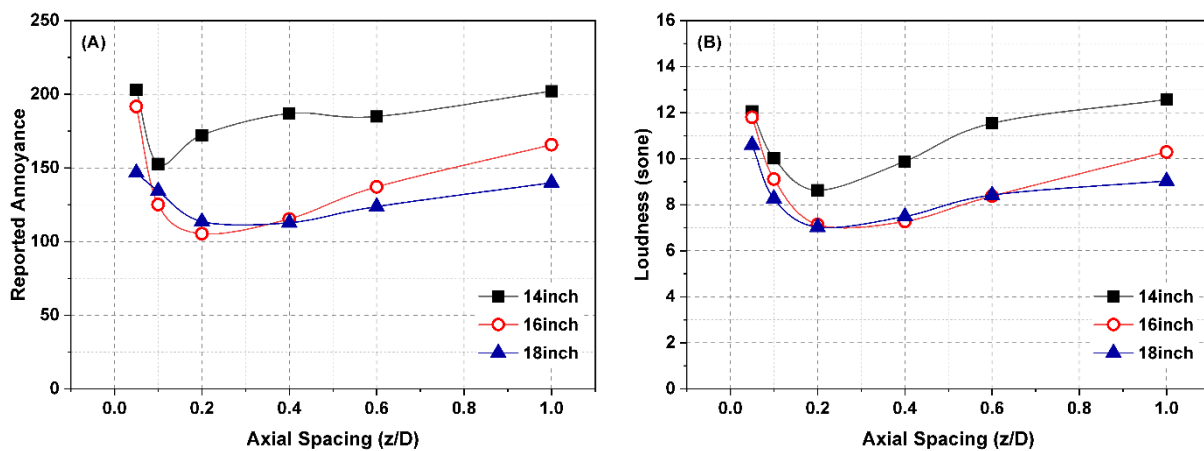
419

420

421 Figure 6 shows the average values (for emission angles of 10 degrees and 85 degrees) of Loudness and
422 reported annoyance (i.e., inter-individual average value) as a function of rotor-rotor axial spacing, for
423 the three combinations of blade diameters in the contra-rotating system (i.e., 14-14 in, 16-16 in and
424 18-18 in). As for the case of the single rotor system, an important reduction in Loudness, and
425 consequently on reported annoyance, is found when the blade diameter increases from 14-14 in to 16-
426 16/18-18 in. Also, as for the grouped analysis presented in Section IV. B, the axial spacing between
427 rotors leading to the lowest values of Loudness and reported annoyance is $z/D = 0.2$. This has been
428 found for the three combinations of blade diameters investigated, except for the reported annoyance
429 for the 14-14 in blade diameter. In this case, the minimum value of reported annoyance is found at
430 $z/D = 0.1$. Exploring the values of the other SQMs, an unusually high value of impulsiveness has

431 been found for this combination of blade diameter at the axial spacing $z/D = 0.2$, which might have
 432 influenced the participants' responses (note that this is an assumption that needs further investigation,
 433 due to the confounding effect of Loudness in the association between Impulsiveness and reported
 434 annoyance). Although this experimental research was carried out for small diameter (low Reynolds
 435 number) rotor blades, impulsiveness has been found to notably contribute to the noise annoyance
 436 caused by helicopter rotor blades (i.e., high Reynolds number)³⁰. This seems to suggest that
 437 impulsiveness might be an important psychoacoustic feature to address noise annoyance of new
 438 rotorcraft vehicles (e.g., VTOL vehicles).

439 It should be noted that due to some issues with the presentation of certain stimuli to the participants
 440 (i.e., $z/D = 0.05, 0.6$ and 1.0 with 16-16 in blade diameter, and $z/D = 0.1$ and 0.2 with 18-18 in blade
 441 diameter), the values displayed for these stimuli in Figure 6 are predicted using the PA model presented
 442 in Section IV. D, rather than directly taken from participants' responses. However, as seen in the
 443 Figure 6, there is a substantial agreement in the trend between predicted and observed values of
 444 annoyance.



445
 446 Figure 6. Loudness (A) and reported annoyance (inter-individual average values) (B) as a function of
 447 rotor-rotor axial spacing for the three blade diameters considered (14-14 in, 16-16 in and 18-18 in)
 448 for the contra-rotating system. Data is displayed is the average value of the emission angles 10

449 degrees and 85 degrees for thrust setting = 16 N. *Note that the unfilled triangles are predicted
450 values using the PA model presented in Section IV. D. (color online)

451 **D. Psychoacoustic annoyance model for rotor noise**

452 Results in the previous sections IV. B and C suggest that the annoyance reported by the participants
453 of this subjective experiment was mainly driven by Loudness. To investigate the contribution of each
454 SQM to the noise annoyance reported for the different rotor noise stimuli, a partial correlation analysis
455 was performed. Table III shows the zero-order (i.e., correlation between variables without controlling
456 for any variable) and partial correlation (when controlling for Loudness) coefficients between the
457 SQMs Sharpness, Aures Tonality, Roughness, Fluctuation Strength and Impulsiveness, and the
458 reported annoyance. Without controlling for Loudness, Sharpness has a substantial negative
459 correlation with annoyance; and Roughness and Fluctuation Strength have a substantial positive
460 correlation with annoyance. However, when controlling for Loudness: (i) as expected, the correlation
461 coefficients for all SQMs decreases, and (ii) Sharpness, Roughness and Impulsiveness have positive
462 correlation coefficients with annoyance. In order words, when controlling for Loudness, an increase
463 in the value of Sharpness, Roughness and Impulsiveness leads to an increase in the reported
464 annoyance. This confirms that the association between the SQMs Sharpness, Aures Tonality,
465 Roughness, Fluctuation Strength and Impulsiveness, and reported annoyance is influenced by
466 Loudness as a confounding factor. Note that interdependencies between Loudness and the remaining
467 SQMs is only for the description of the relationships with reported annoyance, and not between the
468 SQMs and the main design parameters in the rotary systems investigated (which is the main topic of
469 investigation in sections IV.A-C).

470

471 Table III. Zero-order and partial correlation coefficients (controlling for Loudness) between the
 472 SQMs Sharpness, Aures Tonality, Roughness, Fluctuation Strength and Impulsiveness, and the
 473 reported annoyance.

	Sharpness	Aures Tonality	Roughness	Fluctuation Strength	Impulsiveness
Zero-Order	-0.77*	0.11	0.77*	0.78*	-0.29*
Controlling for Loudness	0.21	-0.29*	0.30*	-0.43*	0.24*

474 *Statistically significant (< 0.05)

475

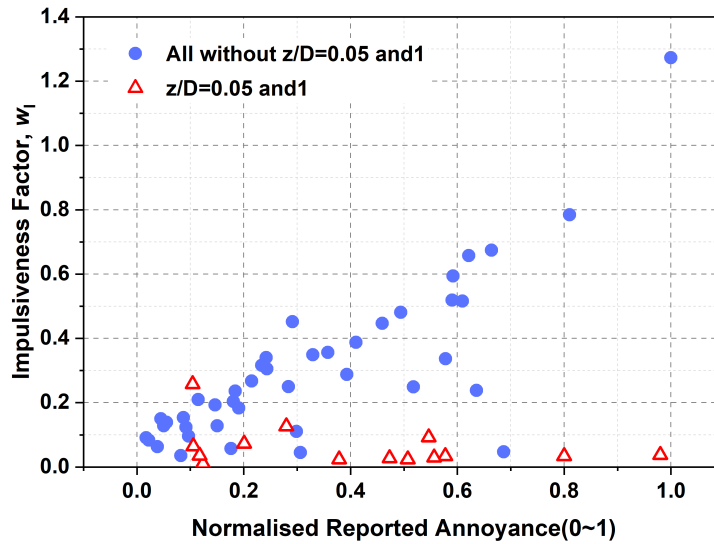
476 As pointed out above, some authors^{15,29} suggest that Impulsiveness and Roughness are likely to
 477 account for the perceptual response to propeller-turbulence interaction noise in rotary systems. None
 478 of the existing PA models include Impulsiveness in their formulation. Zwicker PA model²⁰ accounts
 479 for the relationship between annoyance and Loudness, Sharpness, Fluctuation Strength and
 480 Roughness. Di et al.²¹ and More¹⁹ developed tonality factors to increase the accuracy of PA models
 481 for mechanical sounds in general and aircraft noise respectively.

482 A non-linear regression analysis was performed in IBM SPSS to derive an Impulsiveness factor,
 483 following the same approach of Zwicker PA model²⁰ to derive the factor for Roughness. The
 484 normalised annoyance (0-1 interval) was set as dependent variable, and the Impulsiveness (I) and
 485 Loudness (N) were set at independent variables. The w_I factor is described in Equation 3:

486

487
$$w_I = \frac{0.075 \cdot I}{N^{-1.334}} \quad (\text{Equation 3})$$

488



489

490 Figure 7. Impulsiveness factor (w_I) vs. reported annoyance (normalised to 0-1 interval) for all the
 491 configurations but axial spacings $z/D = 0.05$ and 0.1, and only axial spacings $z/D = 0.05$ and 0.1.
 492 (color online)

493

494 Figure 7 displays a dispersion diagram between the Impulsiveness factor w_I and the reported
 495 annoyance. For rotor-rotor axial spacings $z/D = 0.05$ and 0.1 (closest axial spacings), the reported
 496 annoyance is independent from the value of the Impulsiveness factor w_I . For all the other cases, i.e.,
 497 excluding the axial spacings $z/D = 0.05$ and 0.1, there is a substantial correlation between the
 498 Impulsiveness factor w_I and the reported annoyance ($R^2 = 0.76$). The R^2 coefficient between the
 499 Impulsiveness factor w_I and the reported annoyance for all the configurations is 0.25. These results
 500 are consistent with the relationship between Impulsiveness and axial spacing in contra-rotating
 501 systems (see Figure 3 (F)). Although Loudness is the primary factor driving participants responses of
 502 annoyance for the rotary systems investigated in this research, the Impulsiveness factor (w_I) derived
 503 here can ensure a good prediction of noise annoyance caused by unsteady turbulence in rotary systems.

504 A curve fitting procedure, with the data gathered in the subjective experiment, was used to formulate
505 a new PA model for rotor noise (hereinafter referred to as “Torija et al. PA model”). This model is
506 described in Equation 4.

507

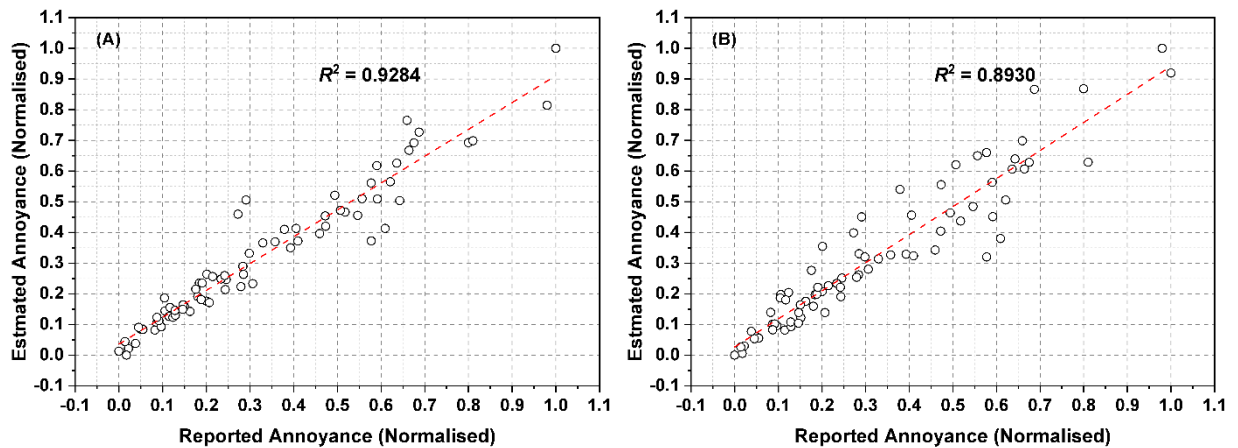
$$508 \quad PA = N_5 \left(1 + \sqrt{\gamma_0 + \gamma_1 w_S^2 + \gamma_2 w_{FR}^2 + \gamma_3 w_T^2 + \gamma_4 w_I^2} \right) \quad (\text{Equation 4})$$

509 where:

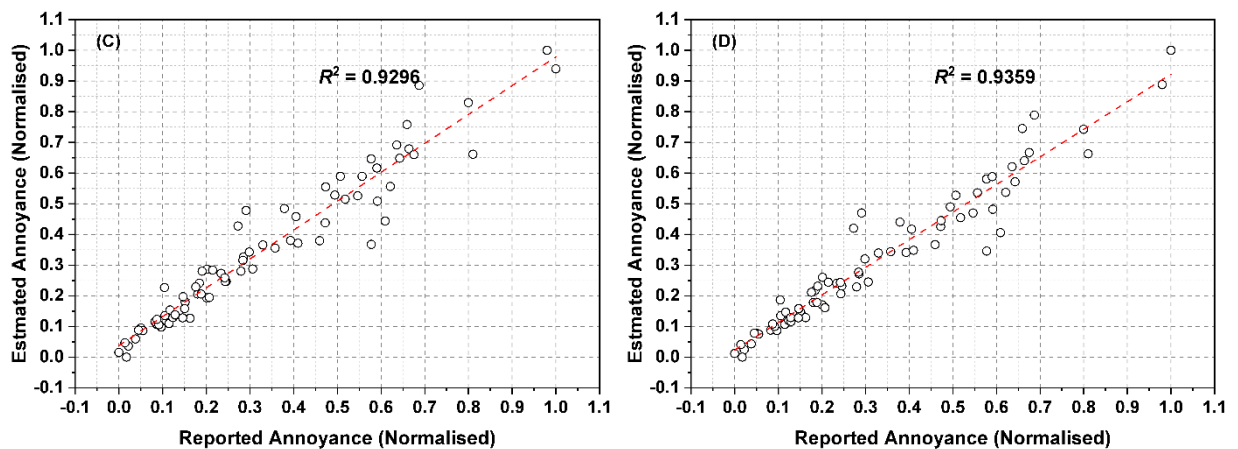
510 N_5 is the 5th percentile of the Loudness metric, w_S^2 and w_{FR}^2 are the factors for Sharpness and
511 Roughness/Fluctuation Strength developed by Zwicker²⁰, w_T^2 is the Tonality factor developed by
512 More¹⁹, and w_I^2 is the Impulsiveness factor presented above. Note that the 5th percentile values of the
513 SQMs have been used to compute all the factors in the PA model. The gamma coefficients in
514 Equation 4 were calculated using a non-linear regression analysis with the reported annoyance as
515 dependent variable and the different factors in Equation 4 as independent variables. The value of
516 these gamma coefficients are: $\gamma_0 = 103.08$, $\gamma_1 = 339.49$, $\gamma_2 = 121.88$, $\gamma_3 = 77.20$ and $\gamma_4 = 29.29$.

517 Figure 8 shows the dispersion diagram between the reported annoyance (i.e., inter-individual average
518 value per test sound) and the annoyance estimated with the PA models: Zwicker²⁰, Di et al.²¹, More¹⁹
519 and Torija et al. (described in Equation 4). As it can be seen, there is a very good agreement between
520 the reported and values of annoyance estimated with all the PA models. The R² values for the
521 estimations with each PA model are (including all test sounds): 0.89 (Di et al.), 0.93 (Zwicker and
522 More) and 0.94 (Torija et al.). The Mean Squared Errors (MSE) of each PA model are: $6.28 \cdot 10^{-3}$
523 (Di et al.), $4.45 \cdot 10^{-3}$ (More), $4.38 \cdot 10^{-3}$ (Zwicker) and $3.92 \cdot 10^{-3}$ (Torija et al.). The
524 achievement of good predictions of annoyance seems to confirm that, in general, the primary factor
525 driving participants’ responses (in this experiment and with these rotor noise stimuli) is Loudness.

526 Table IV shows the R^2 and MSE values of each PA model for both single rotor and contra-rotating
527 test sounds. All the PA models evaluated allow a very good estimation of the reported annoyance, for
528 both the single rotor and contra-rotating test sounds. The performance of the PA models is slightly
529 worse for the contra-rotating test sounds, which might be due to the perceptual effect of more
530 complex phenomena such as potential field interaction tones, beating effects between rotors and
531 turbulence due to interaction effects. For all the cases evaluated, the PA model formulated and
532 presented in this paper (i.e., Torija et al. PA model) achieves slightly better estimations than the other
533 PA models considered. However, the improvement in performance is not significant, as the reported
534 annoyance seems to be mainly driven by loudness (as described above).
535



536



537

538 Figure 8. Reported annoyance (i.e., inter-individual average value per test sound) vs. estimated
 539 annoyance with the PA models: Zwicker (A), Di et al. (B), More (C) and Torija et al. (D) (formulated
 540 in this work). Note that the values of both reported and estimated annoyance are normalised to a 0-
 541 1 interval. (color online)

542

543 Table IV. R² and Mean Squared Error (MSE) values between the reported annoyance and the
 544 annoyance estimated with Zwicker's, Di et al.'s, More's PA models, and Torija et al. PA models.

	Single rotor		Contra-rotating	
	R ²	MSE	R ²	MSE
Zwicker PA model	0.929	$7.29 \cdot 10^{-4}$	0.917	$5.07 \cdot 10^{-3}$
Di et al. PA model	0.900	$1.35 \cdot 10^{-3}$	0.877	$7.20 \cdot 10^{-3}$
More PA model	0.940	$6.73 \cdot 10^{-4}$	0.917	$5.17 \cdot 10^{-3}$
Torija et al. PA model	0.944	$6.39 \cdot 10^{-4}$	0.925	$4.54 \cdot 10^{-3}$

545

546 The curve fitting model formulated in this paper can, however, be very useful to estimate rotor noise
 547 annoyance when loudness is not the dominant factor, or at least, other psychoacoustic factors are as
 548 important as loudness. This might be the case of contra-rotating systems with large rotor-rotor axial
 549 distance, where unsteadiness due to turbulence-propeller interaction leads to high values of
 550 impulsiveness (see Fig. 3 (F)). For the particular case of axial spacings (z/D) from 0.2 to 1.0 and an
 551 emission angle of 85 degrees (lowest emission of potential field interaction tones), the MSE value of
 552 the Torija et al. PA model ($4.98 \cdot 10^{-4}$) is at least half the MSE value of the other three PA models
 553 considered: $7.40 \cdot 10^{-4}$ (Di et al.), $7.64 \cdot 10^{-4}$ (Zwicker) and $1.40 \cdot 10^{-3}$ (More). Of course, further

554 investigation is required to quantify the applicability and overall performance of the curve fitting PA
555 model for the wider range of configurations in rotary systems.

556

557 **V. CONCLUSION**

558 This paper presents the results of a psychoacoustic analysis of a comprehensive database of rotor
559 noise samples encompassing different blade geometries, thrust settings, emissions angles, and single
560 vs. contra-rotating propellers. The results of a listening experiment suggest that the reported
561 annoyance of the rotor sounds evaluated was highly linked to the perceived loudness. Other
562 psychoacoustic factors such as tonality content and high frequency content, low frequency amplitude
563 modulation due to beating effects between rotors, and perceived roughness and impulsiveness due to
564 turbulence caused by interaction effects were analysed and discussed as important contributors to the
565 reported annoyance for the different rotor configurations studied. As a result of the research carried
566 out, a psychoacoustic annoyance model has been formulated and analysed. A curve fitting procedure
567 has been carried out to account for the major psychoacoustic factors influencing rotor noise
568 annoyance investigated in this research. An important contribution is the development of a
569 psychoacoustic function to account for the perceptual effects of impulsiveness. Impulsiveness seems
570 to be an important factor to be considered in the assessment of noise annoyance of new rotorcraft
571 vehicles, including multiple rotors configurations and VTOL transition maneuvers.

572 Further research is needed to encompass more configurations and operating conditions where the
573 perceived loudness is not the main driving factor for annoyance. This research will help to better
574 understand the perceptual effects of other relevant psychoacoustic factors on rotor noise annoyance.

575

576 **ACKNOWLEDGEMENTS**

577 A.J.T. would like to acknowledge the funding provided by Innovate UK and the UK Aerospace
578 Technology Institute (Project number: 73692). P.C. would like to acknowledge the financial support
579 of the Royal Academy of Engineering, United Kingdom (RF/201819/18/194). The authors would
580 also like to thank Dr. Mantas Brazinskas and Dr. Stephen Prior for their efforts in building this rig at
581 the University of Southampton. Z.L. would like to acknowledge the funding from the Natural Science
582 Foundation of Zhejiang University of Science and Technology (No. 2019QN15) and the funding from
583 General Research Project of Zhejiang Provincial Department of Education (No. Y201839836).

584

585 REFERENCES

- 586 1. Brentner KS, Farassat F. Helicopter Noise Prediction: The Current Status and Future
587 Direction. *Journal of Sound and Vibration*. 1994;170(1):79-96.
- 588 2. Romani G, Casalino D. Rotorcraft blade-vortex interaction noise prediction using the Lattice-
589 Boltzmann method. *Aerospace Science and Technology*. 2019;88:147-157.
- 590 3. Brès GA, Brentner KS, Perez G, Jones HE. Maneuvering rotorcraft noise prediction. *Journal*
591 *of Sound and Vibration*. 2004;275(3-5):719-738.
- 592 4. Fields JM, Powell CA. Community reactions to helicopter noise: Results from an experimental
593 study. *The Journal of the Acoustical Society of America*. 1987;82(2):479-492.
- 594 5. Boucher M, Krishnamurthy S, Christian A, Rizzi SA. Sound quality metric indicators of
595 rotorcraft noise annoyance using multilevel regression analysis. 2019.
- 596 6. Gjestland T. Assessment of Helicopter Noise Annoyance: a Comparison Between Noise from
597 Helicopters and from Jet Aircraft. *Journal of Sound and Vibration*. 1994;171(4):453-458.
- 598 7. Gojon R, Jardin T, Parisot-Dupuis H. Experimental investigation of low Reynolds number
599 rotor noise. *The Journal of the Acoustical Society of America*. 2021;149(6):3813-3829.
- 600 8. Zawodny NS, Boyd DD, Burley C. Acoustic Characterization and Prediction of
601 Representative, Small-Scale Rotary-Wing Unmanned Aircraft System Components. 2016.
- 602 9. Torija AJS, Rod H.; Lawrence, Jack L.T. Psychoacoustic Characterisation of a Small Fixed-
603 pitch Quadcopter. Paper presented at: INTER-NOISE and NOISE-CON Congress and
604 Conference Proceedings, InterNoise192019; Madrid, Spain.
- 605 10. Zawodny NS, Boyd DD. Investigation of Rotor-Airframe Interaction Noise Associated with
606 Small-Scale Rotary-Wing Unmanned Aircraft Systems. *Journal of The American Helicopter Society*.
607 2019;65:1-17.
- 608 11. Whelchel J, Alexander WN, Intaratep N. Propeller Noise in Confined Anechoic and Open
609 Environments. In: *ALAA Scitech 2020 Forum*.
- 610 12. Intaratep N, Alexander WN, Devenport WJ, Grace SM, Dropkin A. Experimental Study of
611 Quadcopter Acoustics and Performance at Static Thrust Conditions. In: *22nd ALAA/CEAS*
612 *Aeroacoustics Conference*.
- 613 13. Tinney CE, Sirohi J. Multirotor Drone Noise at Static Thrust. *ALAA Journal*. 2018;56(7):2816-
614 2826.

- 615 14. Luan H, Weng L, Liu R, Li D, Wang M. Axial Spacing Effects on Rotor-Rotor Interaction
616 Noise and Vibration in a Contra-Rotating Fan. *International Journal of Aerospace Engineering*.
617 2019;2019:2125976.
- 618 15. Torija AJ, Chaitanya P, Li Z. Psychoacoustic analysis of contra-rotating propeller noise for
619 unmanned aerial vehicles. *The Journal of the Acoustical Society of America*. 2021;149(2):835-846.
- 620 16. Paruchuri CC, Joseph P, Akiwate DC, Parry AB, Prior SD. On the noise generation
621 mechanisms of overlapping propellers. In: *ALAA AVIATION 2021 FORUM*.
- 622 17. McKay R, Kingan M, Go ST. *Experimental investigation of contra-rotating multi-rotor UAV propeller*
623 *noise*. 2019.
- 624 18. Gwak DY, Han D, Lee S. Sound quality factors influencing annoyance from hovering UAV.
625 *Journal of Sound and Vibration*. 2020:115651.
- 626 19. More S. Aircraft noise metrics and characteristics. *PARTNER Project 24 Report COE-2011*.
627 2011;4.
- 628 20. Zwicker E, Fastl H. *Psychoacoustics: Facts and models*. Vol 22: Springer Science & Business Media;
629 2013.
- 630 21. Di G-Q, Chen X-W, Song K, Zhou B, Pei C-M. Improvement of Zwicker's psychoacoustic
631 annoyance model aiming at tonal noises. *Applied Acoustics*. 2016;105:164-170.
- 632 22. Torija AJ, Clark C. A Psychoacoustic Approach to Building Knowledge about Human
633 Response to Noise of Unmanned Aerial Vehicles. *International Journal of Environmental Research*
634 *and Public Health*. 2021;18(2):682.
- 635 23. Brazinskas M, Prior S, Scanlan J. An Empirical Study of Overlapping Rotor Interference for
636 a Small Unmanned Aircraft Propulsion System. *Aerospace*. 2016;3(4):32.
- 637 24. Torija AJ, Flindell IH. The subjective effect of low frequency content in road traffic noise. *The*
638 *Journal of the Acoustical Society of America*. 2015;137(1):189-198.
- 639 25. De Coensela B, Botteldoorena D, Berglund B, Nilsson ME, De Muer T, Lercher P.
640 Experimental Investigation of Noise Annoyance Caused by High-speed Trains. *Acta Acustica*
641 *united with Acustica*. 2007;93(4):589-601.
- 642 26. Huang Y, Griffin MJ. Comparison of absolute magnitude estimation and relative magnitude
643 estimation for judging the subjective intensity of noise and vibration. *Applied Acoustics*.
644 2014;77:82-88.
- 645 27. Stallen PJ. A theoretical framework for environmental noise annoyance. *Noise and Health*.
646 1999;1(3):69-79.
- 647 28. Berglund MB. . Quality Assurance in Environmental Psychophysics. In: *Ratio scaling of*
648 *psychological magnitude*. Psychology Press; 2013:156-178.
- 649 29. Krishnamurthy S, Christian A, Rizzi S. Psychoacoustic Test to Determine Sound Quality
650 Metric Indicators of Rotorcraft Noise Annoyance. *INTER-NOISE and NOISE-CON Congress*
651 *and Conference Proceedings*. 2018;258(7):317-328.
- 652 30. McMullen AL. *Assessment of noise metrics for application to rotorcraft*, Purdue University; 2014.
653